Optimal Fiducial Points for Pulse Rate Variability Analysis from Forehead and Finger PPG Signals

Elena Peralta[1,2], Jesus Lazaro[1,2,4], Raquel Bailon[1,2], Vaidotas Marozas[3] and Eduardo Gil[1,2]

[1]Biomedical Signal Interpretation and Computational Simulation (BSICoS) Group, Aragon Institute of Engineering Research (I3A), IIS Aragon,University of Zaragoza, Zaragoza, Spain

[2]Centro de Investigacion Biomedica en Red - Bioingenieria, Biomateriales y Nanomedicina (CIBER-BBN), Zaragoza, Spain

[3]Biomedical Engineering Institute and Electronics Engineering Department, Kaunas University of Technology, Kaunas, Lithuania

[4]Department of Biomedical Engineering, University of Connecticut, Storrs, USA

E-mail: elena.peralta.calvo@gmail.com

Abstract.

Objective: The aim of this work is to evaluate and compare five fiducial points for the temporal location of each pulse wave from forehead and finger photoplethysmographic pulse waves signals (PPG) to perform pulse rate variability (PRV) analysis as a surrogate of heart rate variability (HRV) analysis.

Approach: Forehead and finger PPG signals were recorded during tilt-table test simultaneously to the ECG. Artifacts were detected and removed and, five fiducial points were computed: apex, middle-amplitude and foot points of the PPG signal, apex point of the first derivative signal and, the intersection point of the tangent to the PPG waveform at the apex of the derivative PPG signal and the tangent to the foot of the PPG pulse defined as intersecting tangents method. Pulse period (PP) time intervals series were obtained from both PPG signals and compared to the RR intervals obtained from the ECG. Heart and pulse rate variability signals (HRV and PRV) were estimated and, classical time and frequency domain indices were computed.

Main Results: The middle-amplitude point of the PPG signal (n_M), the apex point of the first derivative (n_A^*), and the tangents intersection point (n_T) are the most suitable fiducial points for PRV analysis, which result in the lowest relative errors estimated between PRV and HRV indices, higher correlation coefficients and reliability indexes. Statistically significant differences according to the Wilcoxon test between PRV and HRV signals were found for the apex and foot fiducial points of the PPG, as well as the lowest agreement between RR and PP series according to Bland-Altman analysis. Hence, they have been considered less accurate for variability analysis. In addition, the relative errors are significantly lower for n_M and n_A^* features by using Friedman statistics with Bonferroni multiple-comparison test and, we propose n_M as the most accurate fiducial point. Based on our results, forehead PPG seems to provide more reliable information for a PRV assessment than finger PPG.

Significance: The accuracy of the pulse wave detections depends on the morphology of the PPG. There is therefore a need to widely define the most accurate fiducial point to perform a PRV analysis under non-stationary conditions based on different PPG sensor locations and signal acquisition techniques.

Keywords: Photoplethysmography, PPG, ECG, Heart rate variability, Pulse rate variability, Autonomic nervous system, Fiducial point selection, Transmission and Reflection modes.

1. Introduction

Heart rate variability (HRV) analysis is a non-invasive technique used for the evaluation of the autonomic nervous system (ANS) (TaskForce, 1996) based on the electrocardiogram (ECG) recording. This signal is normally measured using two or more electrodes placed in various positions on the chest and/or limbs. An alternative approach is to estimate pulse rate variability (PRV) from the pulse photoplethysmographic signal (PPG) by simply measuring the changes in the blood flow as changes in the intensity of the light reflected or transmitted through the tissues. The PPG signal is a particularly interesting, simple, low-cost, reliable and comfortable technique for heart rate estimation (Bernardi et al., 1997; Niztan et al., 1998; Allen et al., 2007), where the signal only needs to be acquired from one-single location of the body. Main differences between PRV and HRV are due to physiological factors and to the variability of the location of the PPG fiducial point (Gil et al., 2010). These physiological factors include pulse transit time (PTT), which is the time the pulse wave takes to travel from the heart to the periphery, and the pre-ejection period (PEP), a small delay between the ventricular depolarization and the opening of the aortic valve, also known as isovolumic contraction time. Physiological effects (e.g, respiration) and changing posture cause PTT and PEP to be not constant. All these effects modulate the PPG signal morphology, fiducial points and ultimately PRV. In this sense, this work compares immunity of chosen fiducial points to the changes in PPG signal morphology with the aim to estimate PRV as close to HRV as possible.

Non-invasive optical techniques as PPG can be used to measure the blood volume changes by a few opto-electric components. Typically, a red (630-660 nm) or infrared (800-940 nm) light-emitting diode (LED) is used as light source for illuminating the tissue and, a light detector is used to perform PPG measurements in either transmission or reflection mode. In the transmission mode, LED and photodetector (PD) are placed on opposite sides of the tissues and the light passing through them is measured. In the reflection mode, LED and PD are both facing the same side of the tissues and the light backscattered from them is measured. Reflection mode allows measurements from multiple locations of the body while the backscattered light intensity might be significantly lower in comparison with transmission mode measurements. In recent years, several locations for the PPG sensors have been explored such as finger (Rhee et al., 2001), forehead (Peralta et al., 2017), earlobe (Lu et al., 2009; Vescio et al., 2018), wrist (Grajales et al., 2006; Salehizadeh et al., 2015), chest (Chreiteh et al., 2014), or belly (Spigulis et al., 2005). Wearable pulse rate sensors based on PPG signals have become popular for instantaneous pulse rate assessment (Tamura et al., 2014; Zhang et al., 2014). For clinical purposes, PPG measurements from the earlobe or the forehead can be more

suitable and comfortable to wear (Wang et al., 2007), while ambulatory monitoring systems should be able to detect signals as reliable and stable as possible such as finger PPG measurements (Rhee et al., 2001).

Compared to the ECG signal, the PPG waveform is smooth and it is not characterized by a clearly detectable feature (Rajala et al., 2017). Hence, an important first step for PRV analysis is the accurate detection of the PPG pulse wave and pulse periods (PP). There is therefore a need to widely define the most accurate fiducial point to perform a PRV analysis under non-stationary conditions based on different PPG morphologies and signal acquisition techniques. Different fiducial points for the temporal location of each pulse wave have been proposed in several studies, such as the apex, middle-amplitude and foot points of the PPG signal, maximum of the first and second order derivative PPG signal or tangents intersection point: (Yao et al., 2007) and (Lazaro et al., 2014) from the finger PPG for obstructive sleep apnea diagnosis,(Hemon et al., 2016) from the earlobe PPG for deriving instantaneous pulse rate, or (Rajala et al., 2017) for pulse arrival time measurement. Choosing the most feasible sensor location and measurement technique for PRV analysis may thus be challenging (Buxi et al., 2015).

To the best of our knowledge no study has determined the most suitable and generally accepted PPG measurement technique and fiducial point selection for an accurate pulse detection exploring the possibility of using the PRV signal to evaluate the ANS. Several studies have investigated and verified the accuracy of PRV as a surrogate of HRV (Porto et al., 2009; Charlot et al., 2009; Gil et al., 2010; Khandoker et al., 2011), where results show sufficient accuracy under non-stationary conditions but findings regarding the position of the sensor or the detection algorithm are not conclusive (Schafer et al., 2013).

The main objective of this paper is to determine the most suitable fiducial point to perform a PRV analysis based on the location of the sensor and the PPG measurement technique in non-stationary conditions. The possibility of using PRV extracted from transmission and reflective PPG signals as a surrogate of HRV and to evaluate the changes in ANS elicited by a tilt-table test. To this end, PPG signals acquired from finger and forehead were considered. Reflection-based PPG signals acquired from the forehead are characterized by smoother shapes and the accurate peak detection of the maximum point of the pulse can be challenging, while finger PPG signals may be characterized by a dicrotic notch as the acute drop following the highest single-pulse peak.

2. Materials and Methods

2.1. Data and signal pre-processing

ECG and PPG data were simultaneously collected from 18 young healthy subjects (11 females) by the portable device Cardioholter 6.2-8E78 (KTU BMII, Lithuania). The subjects were instructed to avoid substances influencing cardiovascular system activity

(e.g, alcohol, caffeine) and smoking for 6 hours before the examination. They were normotensive, non-obese and were taking no medication for the duration of the study. Signed, written consent to participate in the study was obtained from all the volunteers, and the ethical principles of the Declaration of Helsinki were followed. Identifiable information was removed from the collected data to ensure participant anonymity. The sampling rates of ECG and PPG signals are $f_s = 500$ Hz and $f_s = 250$ Hz, respectively. For this study, all PPG signals were resampled at 500 Hz. The database includes the conventional 3-lead (I, II, III) ECG data and four PPG signals, at two wavelengths, red (660 nm) and infrared (940 nm), on the finger and on the forehead. Transmission PPG sensor was placed on the right finger and reflection PPG sensor above the left eyebrow on the forehead. In this context, aiming to provide valuable insights to define the best fiducial points for PRV analysis, we are carrying a comprehensive evaluation using two wavelengths and five fiducial points per subject (N=18x2x5) for a robust comparison of the variability signals. All subjects underwent a tilt-table test accomplished by using a tilt table Canaletto Pro (Ferrox S.r.l., Italy), which provokes changes in the ANS. The table is slowly tilted by 80 degrees during 40 seconds. The protocol consisted of three phases: 10 minutes in early supine position (Supine I), 5 minutes head-up tilted (Tilt) and 5 minutes back to supine position (Supine II). Study population characteristics are provided in Table 1.

Table 1: Study population characteristics: age, height, mass and, body mass index.

Age (years)	25.65 ± 2.50
Height (cm)	174.84 ± 9.96
Mass (kg)	67.47 ± 10.67
Body Mass index (kg m^{-2})	21.98 ± 2.27

The pre-processing stage included automatic QRS detection from the ECG signal using a wavelet-based ECG delineator (Martinez et al., 2004). Baseline contamination was removed from the PPG using a high-pass filter with a cut-off frequency of 0.3 Hz, and high frequency noise was attenuated by a low-pass filter with a cut-off frequency of 35 Hz. Zero-phase forward-backward digital filtering was applied in both cases to preserve the pulse morphology.

Artifacts were automatically detected and removed for the variability analysis by an artifact detector based on Hjorth parameters. The algorithm is the result of adapting the algorithm described in (Gil et al., 2008) to non-stationary environments as described in Appendix A. Additional visual inspection of the finger PPG signals revealed the existence of some noisy PPG segments during tilted position, most likely due to motion artifacts. Hence, in addition to the artifact detector, artifacts segments were identified and excluded from the variability analysis from all signals in the database by visual inspection.

2.2. Fiducial points detection

Five fiducial points were computed and compared to perform PRV analysis: apex (n_A), middle-amplitude (n_M) and foot (n_F) of the PPG pulse, apex (n_A^*) of the derivative PPG signal and, intersection point (n_T) of the tangent to the PPG waveform at the apex point n_A^* and tangent to the PPG waveform at the foot point $n_F$defined as intersecting tangents method. The apex points n_A were detected by an automatic pulse detector developed previously in (Lazaro et al., 2014), which detects the upslope point of each PPG pulse (n_A^*) based on a low pass differentiator filter and time-varying threshold.

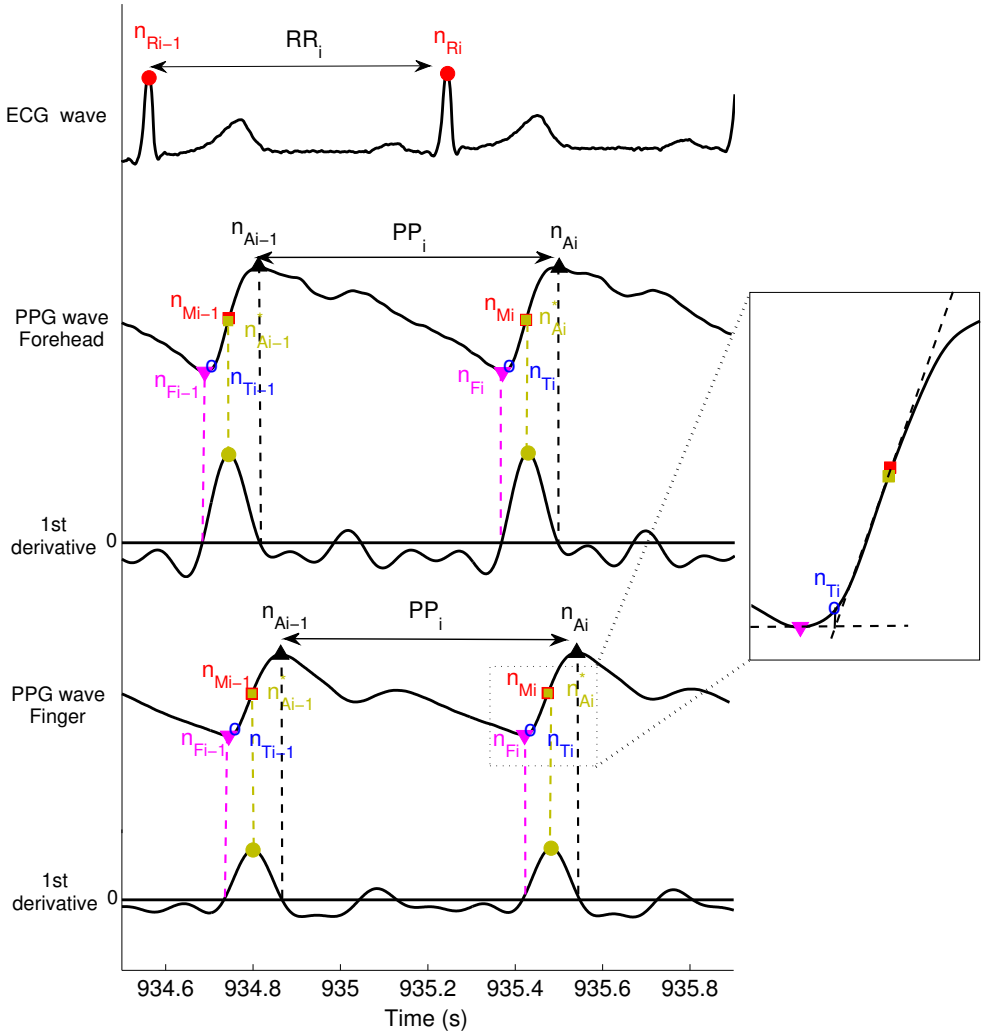

Figure 1: Beat and pulse detection examples. From top to bottom: R waves detected from the ECG, five fiducial points and first derivative signal obtained from the forehead, five fiducial points and first derivative signal obtained from the finger: apex n_A, middle-amplitude n_M and foot $n_F$of the pulse amplitude, apex of the first derivative n_A^* and tangents intersection n_T.

In this paper, in order to better suit the smoother shapes of the reflection-based PPG signals and for a greater robustness under non-stationarity conditions, the apex points n_A were set at the maximum point of the PPG pulses within a time window

starting at n^*_{Ai}, whose length is a half of the median of the three previous instantaneous pulse rate samples ($\hat{m}_{AAi}$):

$$n_{Ai} = \underset{n\epsilon[n^*_{Ai}, n^*_{Ai}+\hat{m}_{AAi}/2]}{\arg\max} \{x(n)\} \tag{1}$$

$$\hat{m}_{AAi} = \text{median } (n^*_{A_{i-4}} - n^*_{A_{i-3}}, n^*_{A_{i-3}} - n^*_{A_{i-2}}, n^*_{A_{i-2}} - n^*_{A_{i-1}}) \tag{2}$$

where $x(n)$ corresponds to the PPG signal. Then, the foot points n_F were set as the minimum point of the PPG pulses within a 250 ms window ending at each n^*_{Ai}:

$$n_{Fi} = \underset{n\epsilon[n^*_{Ai}-0.25f_s, n^*_{Ai}]}{\arg\min} \{x(n)\} \tag{3}$$

The middle-amplitude points n_M were set as the point between n_A and n_F where the amplitude has reached half of the maximum of the pulse amplitude:

$$n_{Mi} = \underset{n\epsilon[n_{Fi}, n_{Ai}]}{\arg\min} \left\{ \left| x(n) - \frac{x(n_{Ai}) + x(n_{Fi})}{2} \right| \right\} \tag{4}$$

Finally, the intersection points $n_T$of the tangent to the PPG waveform at the apex of the derivative PPG signal n^*_A and the tangent to the foot of the PPG pulse $n_F$of gradient zero is estimated as described in (Hemon et al., 2016). The five significant points of the i_{th} PPG pulse computed for PRV analysis are shown in Figure 1 for both forehead and finger PPG signals, as well as the R waves (n_{Ri}) detected for the i_{th} ECG beat as reference.

2.3. Variability analysis indexes

The time difference series between two consecutive R waves from the ECG (RR intervals) and the five fiducial points detected from the PPG (PP intervals) were extracted. Classical time and frequency domain indices from the HRV signal were computed and compared to the indices from the PRV signals. Based on (TaskForce, 1996), the temporal indices studied in this paper are: the mean of heart rate (HRM), standard deviation of all normal-to-normal intervals (SDNN), standard deviation of the successive differences of the NN intervals (SDSD), root mean-square of successive differences of adjacent NN intervals (RMSSD) and, percentage of pairs of adjacent NN intervals differing by more than 50 ms (pNN50). Besides, when performing a frequency analysis, the heart and pulse rate oscillations can be divided into two main bands: low-frequency (LF), 0.04 to 0.15Hz, and high-frequency (HF), 0.15 to 0.4Hz.

The instantaneous pulse rate signal, $x_{PR}(n)$, was obtained from the different pulse time series using a generalization of the integral pulse frequency modulation model and spline interpolation (Mateo et al., 2003). Ectopic beats, missed beats and false detections were identified and corrected (Mateo et al., 2003). Then, the signal $x_{PRM}(n)$ is defined as an estimation of the time-varing mean pulse rate by low-pass filtering the

x_{PR}(n) signal with a cut-off frequency of 0.03 Hz. Finally, the variability signals are defined as the difference:

$$x_{PRV}(n) = x_{PR}(n) - x_{PRM}(n) \tag{5}$$

The Welch's method (Welch et al., 1967) was applied to estimate the power spectral density (PSD) of the $x_{PRV}(n)$ signal using a Hamming window of length 42 seconds with 50% overlap (McNames et al., 2006). Power at each band of interest, P_{LF} and P_{HF}, was computed from the PSD and the $R_{LF/HF}$ ratio and normalized values (P_{LFn} and P_{HFn}) were estimated. A similar procedure was performed to obtain the $x_{HRV}(n)$ signal and related HRV indices.

2.4. Performance evaluation

In each phase of the protocol, HRV and PRV indices have been calculated in short segments whose length is in the range of 1 to 2 minutes due to the nature of the study (McNames et al., 2006; Salahuddin et al., 2007; Baek et al., 2015; Pecchia et al., 2018), where stationarity is assumed and considering a valid segment when there are no artifacts during at least 1 min of PPG signal. Otherwise, that segment is discarded for the variability analysis from all signals in the database. The relative error made in the PRV estimation is calculated for each k_{th} segment and each variability index (I_{PRV} and I_{HRV} for PRV and HRV, respectively) using the HRV signal as reference:

$$E_r(k) = 100 \times \frac{I_{PRV}(k) - I_{HRV}(k)}{I_{HRV}(k)} \qquad k = 1...K, \tag{6}$$

where I: HRM, SDNN, SDSD, RMSSD, pNN50, P_{LF} and P_{HF}.
As a result of this study, the relative errors in terms of median and interquartile range are presented for each variability index among the available segments of all subjects in the database. Besides, absolute errors are presented for the normalized low frequency power, P_{LFn} (P_{HFn}=1-P_{LFn}), and the $R_{LF/HF}$ ratio. These results are separately analyzed for each phase: Supine I, Tilt and Supine II.

The agreement between the RR and PP series was assessed using a Bland-Altman plot (Bland et al., 1986), where the ECG signal is considered as the a gold standard. The bias or average of all differences, the standard deviation around the bias (std) and, the limits of agreement (LOA) defined as bias $\pm$ 1.96 $\times$ std values were computed for each fiducial point.

The data distribution of HRV and PRV parameters was found to be not normal by the Kolmogorov-Smirnov test and, therefore, non-parametric Wilcoxon and Friedman tests were applied. Bonferroni correction for multiple statistical test between the five fiducial points was used to reduce the chances of obtaining false-positive results. In this context, four methodologies were considered to study the reliability and agreement between HRV and PRV signals:

(i) Pearson's correlation coefficient (ρ) was used to measure the linear strength between the variability indices derived from HRV and PRV signals.

(ii) Two reliability indexes were used to measure the interchangeability between measures: Lin's concordance correlation coefficient (CCC, see (Lin et al., 1989)) and intraclass correlation coefficient (ICC, see (Fisher et al., 1925)) .

(iii) Wilcoxon paired-test with Bonferroni correction was used to quantify statistical significance and differences between PRV and HRV signals for the main spectral components within all fiducial points. Then, a second Wilcoxon paired statistical test was performed to evaluate changes in the ANS activity during head-up position with respect to resting position for ECG and PPG signals. In addition, the Cliff's Delta statistics for a non-parametric effect size measure were presented.

(iv) Finally, a test using Friedman statistics with Bonferroni multiple-comparison was applied to assess differences between the estimated relative errors of the five fiducial points.

3. Results

Forehead and finger PPG signals were recorded at two wavelengths, red and infrared. Lower relative errors between HRV and PRV signals were observed for infrared measurements among all fiducial points, especially during tilted position. Besides, major differences were found between both wavelengths in the forehead than in the finger PPG. For instance, the relative errors estimated during supine position for infrared versus red recordings in the forehead PPG were respectively (median/IQR): 18.97/65.90% vs 72.53/157.09% (n_A), 8.48/15.45% vs 17.29/28.57%(n_F), 2.86/4.59% vs 5.33/10.02% (n_M) for the RMSSD index or 6.26/39.43% vs 53.88/299.90 % (n_A), 16.09/17.29% vs 23.23/44.68 % (n_F), 6.84/13.23% vs 6.59/15.37 %(n_M) for P_{HF} . These results suggest that infrared PPG signals are more suitable than red PPG signals in this data. Thus, we focus our analysis to determine the most suitable fiducial point for PRV analysis in the infrared-recorded PPG signals in the rest of the discussion and just those results are presented.

Tables 2 and 3 show the relative errors obtained in the estimation of the time and frequency domain indices derived during tilt-table test for the five fiducial points. Results from finger and forehead PPG are compared to assess the changes in the ANS using HRV indices as reference. These results were obtained by averaging among all subjects the indices presented in section 2.3 in three phases: early supine (Supine I), Tilt and late supine (Supine II). Comparing the results obtained for each fiducial point, higher relative errors in all indices were observed using n_A and n_F , which are more prominent during tilted position. The average percentage of discarded signal during the performance of the PRV analysis was roughly 15% to 20% for all PPG signals. More specifically, the artifact presence per phase (Supine I, Tilt and Supine II) was respectively: 11.9%, 19.3% and 20% in the forehead and 16.33%, 24.67% and 20% in the finger.

Table 2: Time domain PRV analysis. Estimated relative errors between HRV and both PRV signals indices (%). Results shown as *median / interquartile range* values were obtained within all available signal segments for all subjects of the tilt-table test database and for each phase: Supine I, Tilt and Supine II.

		Apex (n_A)		Foot (n_F)		Middle-amplitude (n_M)		First derivative apex (n_A^*)		Tangents intersection (n_T)	
		Forehead	Finger	Forehead	Finger	Forehead	Finger	Forehead	Finger	Forehead	Finger
Supine I	HRM	-0.007 / 0.20	0.004 / 0.09	0.005 / 0.05	0.008 / 0.05	**0.004 / 0.07**	0.007 / 0.041	0.0088 / 0.06	**0.0041 / 0.10**	0.006 / 0.05	0.58 / 0.07
	SDNN	5.26 / 11.32	3.82 / 7.39	2.85 / 3.01	2.52 / 1.95	**1.86 / 2.08**	1.90 / 2.09	2.78 / 2.27	**1.77 / 2.74**	2.80 / 2.64	2.43 / 6.71
	SDSD	18.97 / 65.97	7.98 / 27.11	8.48 / 15.46	5.83 / 5.70	**2.86 / 4.58**	**3.17 / 4.43**	3.90 / 4.28	4.42 / 2.69	6.21 / 10.84	4.40 / 7.53
	RMSSD	18.97 / 65.90	7.98 / 27.12	8.48 / 15.45	5.81 / 5.68	**2.86 / 4.59**	**3.11 / 4.42**	3.90 / 4.28	4.40 / 2.70	6.21 / 10.85	4.40 / 7.55
	pNN50	8.53 / 57.39	4.57 / 19.72	7.80 / 10.42	3.70 / 7.86	**0.044 / 6.16**	**1.49 / 4.63**	3.26 / 3.34	2.83 / 3.51	5.51 / 6.88	3.23 / 5.86
Tilt	HRM	-0.017 / 0.50	-0.14 / 1.03	**0.001 / 0.24**	-0.17 / 0.49	0.024 / 0.12	-0.22 / 0.95	0.016 / 0.27	**0.004 / 0.42**	0.08 / 0.20	0.040 / 0.9
	SDNN	6.65 / 24.47	4.39 / 12.31	3.64 / 5.93	9.54 / 15.39	**3.37 / 3.75**	**-0.59 / 11.04**	3.59 / 4.07	0.78 / 10.83	3.62 / 5.36	3.34 / 24.31
	SDSD	64.33 / 127.70	31.90 / 47.91	17.55 / 34.93	54.31 / 130.03	**5.97 / 18.82**	12.91 / 17.42	8.23 / 16.78	**12.21 / 11.19**	10.89 / 26.85	14.11 / 38.97
	RMSSD	64.06 / 126.89	31.92 / 47.77	17.08 / 34.88	54.23 / 129.76	**5.96 / 18.80**	12.91 / 17.36	8.22 / 16.77	**12.23 / 11.15**	10.89 / 26.85	14.11 / 38.97
	pNN50	27.87 / 78.00	14.78 / 13.83	6.45 / 16.37	31.63 / 57.07	**2.88 / 6.09**	**3.24 / 6.11**	3.26 / 4.36	4.20 / 6.34	3.85 / 8.36	10.42 / 20.64
Supine II	HRM	-0.065 / 0.75	-0.03 / 0.40	**-0.001 / 0.14**	-0.0204 / 0.62	-0.009 / 0.22	**-0.001 / 0.57**	0.0029 / 0.33	-0.24 / 0.60	0.002 / 0.18	-0.10 / 0.62
	SDNN	5.19 / 12.24	0.40 / 4.54	2.17 / 3.09	2.92 / 7.36	**0.88 / 5.13**	**2.04 / 3.84**	2.26 / 2.94	2.54 / 3.38	2.01 / 3.26	2.51 / 3.45
	SDSD	22.84 / 107.76	12.24 / 22.66	11.92 / 15.68	13.78 / 19.70	**7.30 / 9.53**	**7.67 / 11.24**	7.33 / 6.75	10.33 / 8.45	8.62 / 10.21	10.88 / 15.36
	RMSSD	22.85 / 107.62	12.20 / 22.71	11.94 / 15.63	13.73 / 19.64	**7.29 / 9.59**	**7.68 / 11.22**	7.33 / 6.77	10.30 / 8.45	8.62 / 10.21	10.87 / 15.36
	pNN50	18.21 / 49.61	6.04 / 11.14	4.91 / 7.45	5.65 / 13.60	**1.94 / 5.21**	**2.13 / 6.84**	3.79 / 6.30	4.17 / 5.37	4.36 / 6.75	4.23 / 6.13

*The minimum errors obtained for each variability index in the forehead and in the finger within all fiducial points are bold.

Table 3: Frequency domain PRV analysis. Estimated relative (P_{LF}, P_{HF}) and absolute (P_{LF_n}, $R_{LF/HF}$) errors between HRV and both PRV signals indices (%). Results shown as *median / interquartile range* values were obtained within all available signal segments for all subjects of the tilt-table test database and for each phase: Supine I, Tilt and Supine II.

		Apex (n_A)		Foot (n_F)		Middle-amplitude (n_M)		First derivative apex (n_A^*)		Tangents intersection (n_T)	
		Forehead	Finger	Forehead	Finger	Forehead	Finger	Forehead	Finger	Forehead	Finger
Supine I	P_{LF}	4.32 / 22.84	7.33 / 25.50	**4.06 / 9.76**	6.17 / 7.44	5.27 / 7.95	**5.88 / 7.87**	5.45 / 9.42	6.84 / 4.91	6.35 / 12.15	6.65 / 4.14
	P_{HF}	6.26 / 39.43	16.57 /173.80	16.09 / 17.29	15.54 / 25.03	6.84 / 13.23	7.08 / 12.50	12.71 / 12.86	11.80 / 11.63	14.65 / 16.76	12.47 / 23.79
	P_{LF_n}	-0.10 / 1.84	-0.07 /0.74	-0.26 / 0.82	**-0.05 / 0.73**	**-0.06 / 0.49**	-0.08 / 0.44	-0.24 / 0.49	-0.08 / 0.39	-0.24 / 0.57	-0.07 / 0.46
	$R_{LF/HF}$	-0.11 / 2.02	-0.07 / 0.80	-0.27 / 0.91	-0.05 / 0.81	-0.07 / 0.53	-0.09 / 0.46	-0.26 / 0.55	-0.08 / 0.42	-0.26 / 0.63	-0.07 / 0.52
Tilt	P_{LF}	15.08 / 14.90	2.55 / 58.41	**5.07 / 15.14**	18.47 / 396.46	9.60 / 11.68	**2.18 / 23.54**	13.60 / 14.84	5.75 / 43.19	12.55 / 14.81	10.61 / 79.01
	P_{HF}	62.08 / 156.67	71.76 / 49.28	36.69 / 82.76	132.82 / 744.64	**23.35 / 37.07**	23.56 / 30.10	38.87 / 24.61	**22.86 / 27.45**	34.82 / 79.83	39.12 / 217.42
	P_{LF_n}	-9.52 / 11.38	-5.49 / 8.81	-3.91 / 5.69	-4.44 / 10.41	-1.50 / 2.05	**-2.67 / 8.54**	**-1.31 / 2.96**	-3.77 / 7.34	-1.98 / 3.66	-3.95 / 8.14
	$R_{LF/HF}$	-12.49 / 14.58	-7.00 / 11.00	-4.47 / 9.07	-5.28 / 14.90	-1.92 / 3.61	**-4.26 / 12.94**	**-1.77 / 5.07**	-4.77 / 9.83	-2.37 / 6.17	-4.90 / 11.43
Supine II	P_{LF}	5.05 / 48.87	4.43 / 26.38	**1.84 / 17.28**	4.62 / 17.35	1.89 / 17.94	3.23 / 10.34	9.79 / 30.74	**2.36 / 25.03**	5.32 / 21.05	4.28 / 18.49
	P_{HF}	29.51 /213.42	20.33 / 73.77	30.85 / 37.48	25.85 / 58.94	6.56 / 53.70	9.39 / 24.89	18.78 / 44.96	14.67 / 36.12	23.91 / 39.28	21.96 / 49.53
	P_{LF_n}	-0.09 / 2.53	-0.02 / 1.22	-0.28 / 1.53	-0.40 / 1.49	**-0.09 / 1.29**	**-0.084 / 0.96**	-0.22 / 0.90	-0.09 / 1.11	-0.24 / 1.06	-0.22 / 1.23
	$R_{LF/HF}$	-0.09 / 2.63	-0.02 / 1.30	-0.28 / 1.71	-0.41 / 1.68	**-0.09 / 1.40**	**-0.08 / 1.04**	-0.23 / 1.03	-0.09 / 1.17	-0.24 / 1.19	-0.29 / 1.40

*The minimum errors obtained for each variability index in the forehead and in the finger within all fiducial points are bold.

Figure 2 shows Bland–Altman plots that evaluate the discrepancies between RR series obtained from the ECG and all PP series obtained from PPG measurements and the stability across a wider value range. The central, the upper and lower horizontal dash lines show the bias (mean) and the LOA (bias ± 1.96 × std values) of the differences between methods, respectively. Exact values of bias, standard deviation and LOA are shown on top of each figure, where a total of 26361 paired RR and PP measurements were used for the analysis. For n_A the discrepancies are higher and, in general, for the measurements in the finger.

Pearson's correlation between HRV and PRV signals was quantified for $P_{LF}$and P_{HF}. Significant and positive linear correlation ($\rho > 0.9$) was found in both indices during tilted position using n_F, n_M, $n_A^*$and $n_T$for the forehead PPG and using n_M, $n_A^*$and $n_T$for the finger PPG as shown in Table 4. In addition, we consider CCC and ICC coefficient values lower than 0.7 as markers of poor reliability between HRV and PRV signals. In this sense, $n_A$in the forehead or $n_A$and $n_F$in the finger provide the lowest values.

Table 4: Pearson's correlation (ρ) and reliability coefficients (CCC, ICC) between HRV and PRV signals for P_{LF}, $P_{HF}$and for each phase: Supine I, Tilt and Supine II.

			Forehead					Finger				
			n_A	n_F	n_M	n_A^*	n_T	n_A	n_F	n_M	n_A^*	n_T
Supine I	P_{LF}											
		ρ	**0.96**	**0.99**	**0.99**	**0.99**	**0.99**	**0.95**	**0.99**	**0.99**	**0.99**	**0.98**
		CCC	**0.94**	**0.99**	**0.99**	**0.99**	**0.99**	**0.94**	**0.99**	**0.99**	**0.99**	**0.99**
		ICC	**0.97**	**0.99**	**0.99**	**0.99**	**0.99**	**0.97**	**0.99**	**0.99**	**0.99**	**0.99**
	P_{HF}											
		ρ	0.85	**0.99**	**0.99**	**0.99**	**0.99**	**0.920**	**0.99**	**0.99**	**0.99**	**0.99**
		CCC	0.78	**0.98**	**0.99**	**0.99**	**0.99**	0.89	**0.99**	**0.99**	**0.99**	**0.99**
		ICC	0.88	**0.99**	**0.99**	**0.99**	**0.99**	**0.95**	**0.99**	**0.99**	**0.99**	**0.99**
Tilt	P_{LF}											
		ρ	0.82	**0.98**	**0.98**	**0.99**	**0.99**	**0.96**	0.36	**0.93**	0.78	0.77
		CCC	0.79	**0.96**	**0.95**	**0.96**	**0.97**	**0.95**	0.10	**0.91**	0.77	0.70
		ICC	0.89	**0.98**	**0.98**	**0.98**	**0.98**	**0.98**	0.06	**0.96**	0.88	0.86
	P_{HF}											
		ρ	-0.06	**0.96**	**0.98**	**0.99**	**0.99**	0.66	**0.92**	**0.90**	**0.91**	**0.92**
		CCC	-0.09	0.64	0.88	**0.91**	0.85	0.46	0.004	0.80	0.83	0.86
		ICC	-0.15	0.78	**0.93**	**0.95**	**0.93**	0.58	0.004	0.89	**0.91**	**0.92**
Supine II	P_{LF}											
		ρ	**0.96**	**0.98**	**0.98**	**0.98**	**0.98**	**0.97**	**0.90**	**0.97**	**0.95**	**0.94**
		CCC	**0.95**	**0.96**	**0.95**	**0.96**	**0.96**	**0.97**	0.53	**0.93**	0.74	0.70
		ICC	**0.97**	**0.98**	**0.97**	**0.98**	**0.98**	**0.98**	0.70	**0.96**	0.85	0.81
	P_{HF}											
		ρ	0.89	**0.92**	**0.98**	**0.97**	**0.93**	**0.90**	**0.90**	**0.95**	**0.99**	**0.98**
		CCC	0.85	0.88	**0.98**	**0.94**	**0.91**	0.87	0.86	**0.94**	**0.98**	**0.97**
		ICC	**0.92**	**0.93**	**0.99**	**0.97**	**0.94**	**0.93**	**0.93**	**0.97**	**0.99**	**0.99**

*Values higher than 0.9 are bold

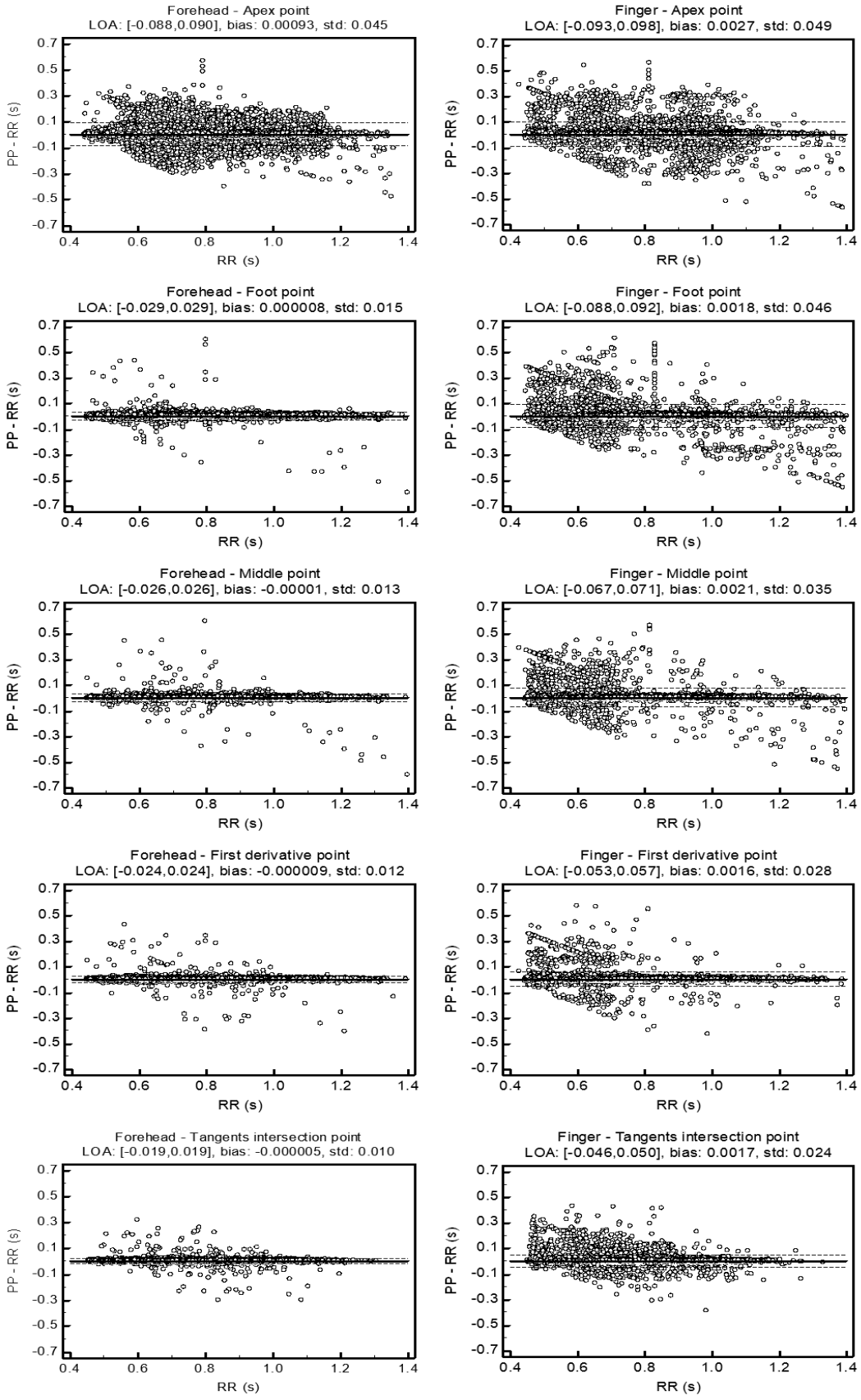

Figure 2: Bland-Altman plots comparing paired RR and PP series obtained from forehead (right) and finger (left) PPG signals within all fiducial points for all subjects. Bias and limits of agreement (bias $\pm$ 1.96 $\times$ std values) are shown in solid and dash lines, respectively.

Statistically significant differences were found between HRV and PRV signals during tilted position according to the Wilcoxon paired-test as shown in Figure 3, using the Bonferroni correction for a multiple-comparison. In particular, significant differences (p-value < 0.01) were found in P_{HF} between forehead PRV and HRV using n_A and, between finger PRV and HRV using n_A, n_F and n_T.

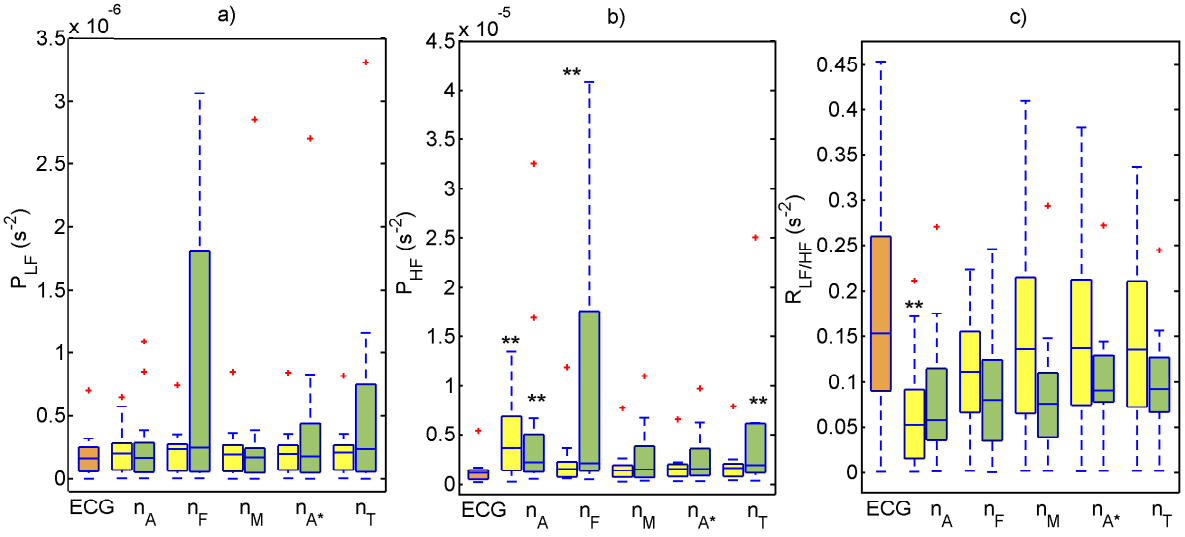

Figure 3: Inter-subject medians of (a) P_{LF}, (b) P_{HF} and (c) $R_{LF/HF}$ ratio from ECG (orange bars), forehead PPG (yellow bars) and finger PPG (green bars) for each fiducial point during head-up tilted position. The outliers are plotted individually using red markers ('+'). Significant differences (p-value < 0.01) according to the Wilcoxon paired statistical test are denoted between compared groups (ECG/Forehead and ECG/Finger) with (**)

During head-up tilted position, the relative errors are significantly higher in P_{HF} using n_A in the forehead and, in P_{LF} and P_{HF} using n_F in the finger compared to n_M and n_A^* fiducial points according to the Friedman statistics with Bonferroni multiple-comparison test (see Figure 4). In addition, during early and late supine, it can be observed that the relative errors in P_{HF} are significantly lower using n_M compared to other fiducial points.

Table 5: The p-value obtained by the Wilcoxon paired-test between compared pairs (Supine I/ Tilt and Supine II/Tilt) for ECG and both PPG signals. Effect size is shown in brackets.

		ECG		Forehead		Finger	
		SupI/Tilt	SupII/Tilt	SupI/Tilt	SupII/Tilt	SupI/Tilt	SupII/Tilt
n_M	P_{LF}	**0.032** (0.43)	0.062 (0.37)	**0.030** (0.43)	0.085 (0.34)	**0.023** (0.30)	**0.042** (0.27)
	P_{HF}	0.091 (0.34)	**0.023** (0.46)	0.28 (0.21)	**0.042** (0.41)	0.37 (0.20)	0.26 (0.25)
	$R_{LF/HF}$	**0.001** (0.64)	**0.002** (0.60)	**0.001** (0.66)	**0.003** (0.58)	**0.009** (0.59)	**0.005** (0.56)
n_A^*	P_{LF}	**0.032** (0.39)	0.062 (0.38)	**0.038** (0.41)	0.053 (0.39)	**0.021** (0.30)	**0.042** (0.27)
	P_{HF}	0.091 (0.34)	**0.023** (0.44)	0.17 (0.28)	**0.023** (0.46)	0.32 (0.22)	0.175 (0.30)
	$R_{LF/HF}$	**0.001** (0.64)	**0.002** (0.60)	**0.001** (0.68)	**0.001** (0.63)	**0.002** (0.64)	**0.003**(0.54)

*p-values lower than 0.05 are bold.

Results of the Wilcoxon paired test comparing changes in the ANS activity during head-up position with respect to resting position are presented in Table 5 for the pairs Supine I / Tilt and Supine II / Tilt. It was observed that HRV and PRV signals present similar results using n_M and n_A^* but not for the rest, so just those fiducial points results are presented. Besides, large effect sizes (ES) show that differences in HRV or PRV between the phases of the tilt-table test are more important than the differences between HRV and PRV signals (ES < 0.1 in P_{LF} and ES < 0.2 in P_{HF} during supine position or ES < 0.20 in P_{LF} and ES < 0.30 in P_{HF} using n_M, n_A^* and n_T during tilted position).

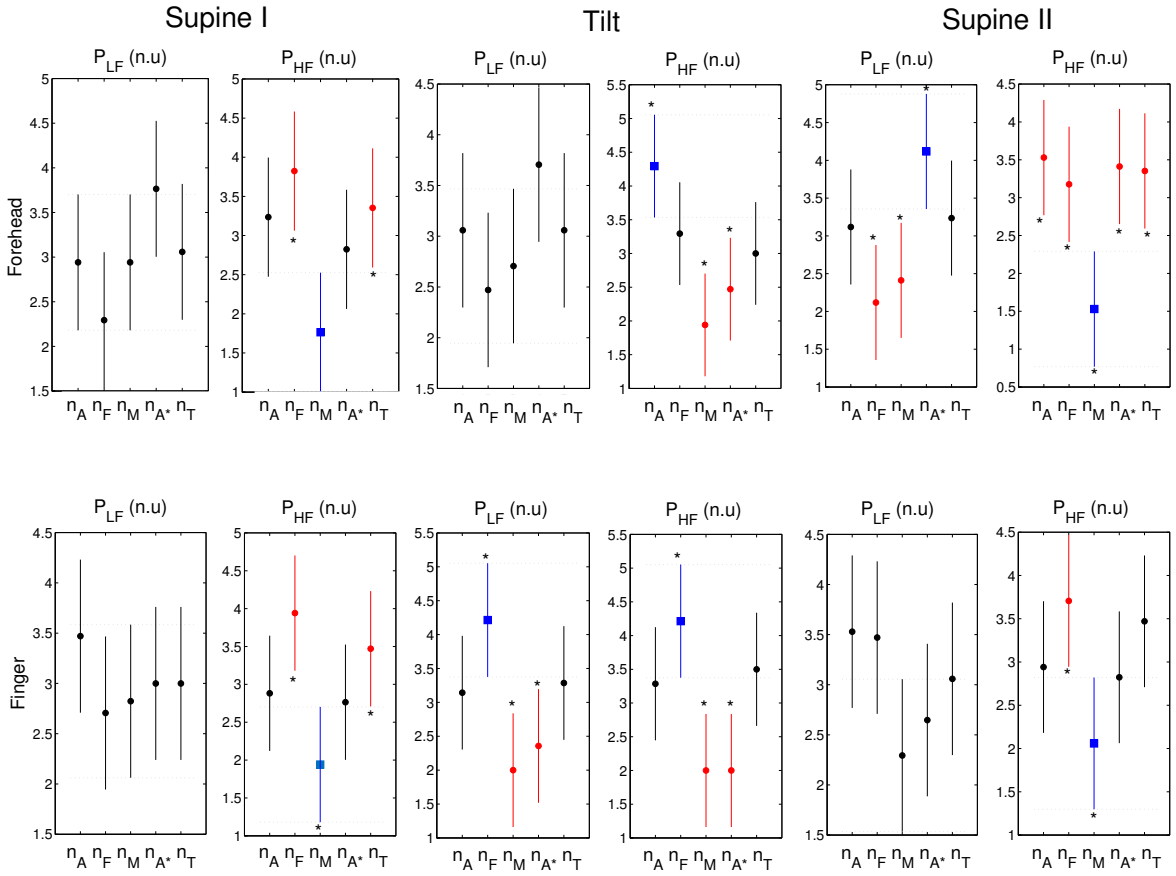

Figure 4: Mean values of P_{LF} and P_{HF} relative errors obtained in the estimation of PRV indices using HRV as reference. Results are shown for each fiducial point during early supine, tilt and late supine in the forehead (top) and finger (bottom) PPG signals. (*) indicates statistically significant differences between compared groups by using Friedman statistics with Bonferroni multiple-comparison test when the mean value of one fiducial point (blue) is significantly higher or lower than other(s) (red).

4. Discussion

In this work, we analyze the most accurate fiducial points for PRV analysis as a surrogate for HRV under non-stationary conditions in young healthy subjects. For this purpose, five fiducial points were computed and their suitability for PRV analysis are compared based on the location of the sensor, forehead and finger, and two PPG measurement techniques, reflection and transmission modes. First, the classical time and frequency variability indices were estimated for each fiducial point in the three phases of the tilt table test. In order to measure P_{LF} and P_{HF} , at least 1 minute of HRV and PRV signals is needed (Pecchia et al., 2018). Therefore, due to the nature of this study, the length of the segments and the Hamming window were chosen to provide a reliable estimation of the P_{LF} power (McNames et al., 2006; Baek et al., 2015) and an accurate comparison between the variability signals. Second, statistical differences are quantified between PRV and HRV indices within each fiducial point and to evaluate changes in the ANS provoked during the tilt-table test with respect to baseline conditions.

Several studies have indicated differences sufficiently small to suggest the use of PRV as an alternative measurement of HRV (Gil et al., 2010; Khandoker et al., 2011). It has been pointed out that PRV can be used to discriminate sleep apneic and non-apneic decreases in the amplitude fluctuations of the PPG signal without introducing any additional signal (e.g, ECG), Lazaro et al. (2014). Hence, PPG signals take special relevance in sleep studies because there is no need of using many sensors which could disturb the physiological sleep.

Our results suggest that infrared PPG signals are more suitable than red PPG signals in this data. However, the wavelength of the used light affects the acquired PPG signal quality in several ways. On one hand, the interaction of the hemoglobin with the light depends on the wavelength. Most of the hemoglobin in arteries is oxygenated and the absorption coefficient of oxygenated hemoglobin in infrared is higher than in red. Therefore, the AC component of the infrared PPG signal is expected to have a higher dynamic range, which may reduce the error in fiducial points locations, making infrared PPG signal more convenient than the red one. On the other hand, shorter wavelengths penetrate less than the longer wavelengths, leading to measures that are more affected by the local tissues and less corrupted by the ambient light. However, the light has to penetrate deep enough to interact with arterial vessels so a too short wavelength is not convenient either. Furthermore, the melanin has a huge interaction with the light, making the optimal wavelength choice to be dependent on the type of the skin of the subject. The superposition of all these effects leads to higher signal quality using red or infrared and, in this case, our observation is that infrared is more convenient than red in accordance to (Fallow et al., 2013), where infrared PPG signals are reported to have a higher signal-to-noise ratio than red PPG signals when measuring on white skins.

4.1. Variability estimation accuracy

The accuracy of the PRV estimation highly depends on the technique used to acquire the signal, the possible signal interferences or artifacts, and the morphology of the PPG signal according to the recording methodology and sensor location on the body. In line with other studies (Schafer et al., 2013; Peng et al., 2015), our results show higher relative errors between PRV and HRV for RMSSD or SDSD variability indices than for SDNN. Also, low-frequency indices are better aligned than high-frequency indices between both variability signals (Gil et al., 2010).

Time domain. Time domain indices derived from forehead and finger PRV signals present a small relative error during supine position, with values lower than 8%, 10%, 11% for n_M, n_A^*, and n_T fiducial points, respectively. It has been shown that in short-term variability related indices, such as SDSD and RMSSD, the relative errors are higher during tilted position than during supine interval, with values lower than 15% for these three fiducial points. Moreover, it should be noticed that higher relative errors are obtained for n_A and n_F during both supine and tilted positions. The global results suggest that PRV analysis could be used as a surrogate measurement of HRV analysis especially in the forehead PPG signals, with relative errors of 6%, 8% and 11% (n_M, n_A^* and n_T) compared to 12%, 13% and 14% in the finger PPG signals.

Frequency domain. Frequency domain indices derived from both PRV signals present relative errors lower than 25% during supine position in P_{LF} and P_{HF}, with values lower than 6%, 10% or 7% in P_{LF} and 10%, 19% or 24% in P_{HF} for n_M, n_A^* and n_T fiducial points, respectively. The relative errors present higher variance during head-up position, especially in P_{HF} and $R_{LF/HF}$ ratio. For instance, for finger PPG signals (median/IQR): 2/23%, 6/43% and 10/80% (n_M, n_A^* and n_T) in P_{LF} and 24/30%, 23/27%and 40/217% in P_{HF} compared to 10/11%, 13/14% and 13/15% in P_{LF} and 24/37%, 39/25% and 35/80% in P_{HF} for the forehead PPG. Due to the small values obtained in P_{HF} for the reference HRV, the relative errors for HF-related indices during head-up position could be higher than expected according to the relative error estimation defined in Equation 6. In line with the time domain related indices results, higher relative errors are observed for n_A and n_F during supine and tilted positions.

In general, the relative errors are slightly lower for the reflection-based PPG signals measured in the forehead than for the transmission-based PPG signals measured in the finger, in particular during head-up position. Besides, one of the most important limitations of PPG signals for PRV analysis are motion artifacts. Their effect has been investigated during this study, where approximately 15% of the forehead PPG signals was considered artifact and discarded for the PRV analysis while 20% of the finger PPG signals was discarded. This analysis suggests that forehead PRV signals could provide more reliable information under non-stationary conditions while finger PRV signals can be more affected by motion artifacts.

4.2. Statistical analysis

The Bland-Altman plots between RR and PP series exhibited a close agreement between measures, where the estimated bias is below 0.002 for all cases. The analysis shows a larger divergence in the finger than in the forehead measurements. More specifically, the limits of agreement in the forehead were below [-0.03,0.03] for n_M, n_A^* and n_T. Pearson's correlation between HRV and both PRV signals show a significant and positive linear relationship ($\rho > 0.9$) during early supine for all fiducial points except n_A in the forehead PPG. Besides, strong correlation during tilted position is observed for all fiducial points except n_A between HRV and forehead PRV indices and for n_M, n_A^* and n_T between HRV and finger PRV. Weaker correlation coefficients as well as higher relative errors presented in Tables 2 and 3 suggest that n_A is not an accurate feature for a PRV analysis in the forehead, as is located at smooth zones of the PPG morphology and its location can be affected by a low level of noise.

The Wilcoxon paired-test using the Bonferroni correction was performed to corroborate our assumptions. No statistically significant differences were found during early or late supine position between HRV and PRV signals in the finger and in the forehead. Figure 3 shows that statistically significant differences (p-value < 0.01) were found between PRV and HRV signals for the pair ECG/Finger using n_A, n_F and n_T during head-up position in P_{HF}, and for the pair ECG/Forehead using n_A. It is well known that an accurate pulse detection is crucial in PRV analysis, thus these results suggest that the apex and foot points of the PPG pulse are less accurate for a PRV analysis among different PPG morphologies.

In order to verify which fiducial point can be more suitable for PRV analysis, statistically significant differences between compared groups were analyzed by using Friedman statistics with Bonferroni multiple-comparison test. During early and late supine, the relative errors in P_{HF} are significantly lower for n_M compared to n_F and n_T (Figure 4), with relative errors of 6% compared to 20% or 30% as shown in Table 3 for Supine II. On the other hand, significantly higher errors during tilt in P_{HF} are observed for n_A in the forehead PPG as well as in P_{LF} and P_{HF} for n_F in the finger PPG compared to n_M and n_A^*. These results confirm that the apex and foot points of the PPG pulse seem to be less accurate for a PRV analysis, with the lowest reliability indexes and wider LOA in n_A for the forehead PPG and in n_F for the finger PPG. Strong correlation (ICC > 0.9) and a narrower LOA indicate that the PP series obtained from the middle-amplitude point and the apex point of the first derivative are interchangeable with the RR series to assess a variability analysis.

Finally, a second Wilcoxon test was performed to evaluate changes in the ANS activity during tilted position with respect to baseline conditions for ECG and PPG signals. It is shown that there are statistically significant differences between the pairs Supine I / Tilt in P_{LF} and Supine II / Tilt in P_{HF}. It should be noted that HRV and forehead PRV signals present similar results using n_M and n_A^* fiducial points, therefore same HRV and PRV physiological interpretation can be assumed. In addition, HRV and

finger PRV signals present similar results for both fiducial points for the pair Supine I / Tilt but not for the pair Supine II / Tilt in P_{HF}, which could be due to the transit of ANS recovery following orthostatic stress. Consequently, PRV could be used to evaluate ANS activity under non-stationary conditions based on the PPG pulses detected in the middle-amplitude point and the apex point of the first derivative.

4.3. Fiducial points selection

The apex n_A is probably the most common fiducial point used to calculate PP intervals. Its location in the forehead PPG is normally at smooth zones where a low level of noise can significantly change its temporal location. The relative errors obtained in the PRV indices compared to the HRV using the apex n_A are the highest ones of the five fiducial points presented and statistically significant differences were found between HRV and both PRV signals. Previously in Figure 1, the smoother shapes of the reflection-based PPG waveforms were analyzed and these results confirm that the apex n_A is not the most suitable point for a PRV analysis due to its minor robustness, especially from forehead PPG signals. The accuracy of the foot point n_F for PPG pulse detections depends on the morphology of the PPG pulse. The relative errors obtained in the PRV indices estimation during tilt position for this point are higher than for others fiducial points and in particular, for the transmission-based PPG signals in the finger. Results presented in Tables 2 and 3 show that the middle-amplitude point n_M, the apex point of the first derivative n_A^*, and the tangents intersection point n_T are the most suitable fiducial points for a PRV analysis, particularly during head-up tilted position related to a sympathetic activation of the ANS. The middle-amplitude point of AC component of PPG signal, n_M, is located at the systolic slope of the PPG pulse, which is an abrupt zone and therefore it is more robust against noise in all kind of PPG morphologies. This point is measured from the PPG signal itself and it is computationally efficient. The PPG derivative signal is characterized by a sharp and well-defined peak n_A^* above the noise floor which is again easy to detect. Although, its physiological interpretation and time-relation to the ECG signal could be more difficult to analyze. The intersecting method, which defines n_T, is the highest computationally demanding method. It depends on other two fiducial points (n_F and n_A^*) and the inaccurate detection of one point could be compensated by the other one.

In accordance with our results, in (Rajala et al., 2017) the apex point of the first derivative was considered the most promising fiducial point to be used in pulse arrival time while in (Hemon et al., 2016) for ear-PPG and (Posada-Quintero et al., 2013) for finger-PPG the correlation between PPG and ECG for a PRV analysis under stationary-conditions was greatest for the intersecting tangents method followed by the apex of the first derivative. To the best of our knowledge, there are no previous studies which define the most accurate fiducial point to perform a PRV analysis under non stationary-conditions and, which consider the possible artifacts impact for different PPG morphologies. Based on our results, n_M, n_A^* and $n_T$can be used for PRV analysis and we

propose the middle-amplitude point of the PPG as the most accurate one under different PPG morphologies and sensor locations, obtaining statistically significant lower relative errors in $P_{LF}$and P_{HF}within all fiducial points as shown in Figure 4 and in Tables 2 and 3.

4.4. Limitations

One potential limitation of this study is the fact that our database consists of mostly young, healthy individuals. Due to the limited number of subjects in the database and the major presence of artifacts in the transmission-based PPG signals acquired from the finger, a further study should validate the forehead and finger PPG signals suitability for PRV analysis in a comprehensive sample set. Second, the signals in this study were acquired in a well-controlled experiment and motion artifacts were substantially suppressed. In real scenarios, motion artifacts can be more disturbing. In addition, the transmission PPG sensor was placed on the right finger in this study. According to (Yeragani et al., 2007), there was no significant difference between right and left side of the body to measure PPG signals in normal controls. However, it is an interesting point to address in a future work.

5. Conclusion

The middle-amplitude point, the apex point of the first derivative and the tangents intersection point variability-related indices present the lowest relative errors estimated between PRV and HRV indices and the highest correlation and agreement coefficients. Our results indicate that these fiducial points can be more suitable for PRV analysis and we propose the middle-amplitude point of the PPG as the most accurate one under non-stationarity conditions based on two different locations of the sensor, forehead and finger, and two PPG measurements techniques, reflection and transmissions modes, considering the possible impact of artifacts presence. This point is one of the most efficient in terms of computation and statistically significant lower relative errors were observed in P_{LF} and P_{HF}within all fiducial points.

In general, the relative errors are lower for the forehead PPG than for the finger PPG. Besides, the physiological interpretation to evaluate changes in the ANS activity during head-up tilted position respect to resting position showed similar results between HRV and forehead PRV for the middle-amplitude point and the apex point of the first derivative. These findings suggest that forehead PPG signals could provide more reliable PRV information than finger PPG under non-stationary conditions.

6. Acknowledgement

This work was supported by Government of Aragon and European Social Fund (EU) through Grupo de Referencia BSICoS (T39 17R), by University of Zaragoza (UZ2018-TEC-05) and by CIBER in Bioengineering, Biomaterials & Nanomedicine

(CIBER−BBN) through Instituto de Salud Carlos III. This work was partially supported by the Research Council of Lithuania (Agreement No. S-MIP-17/81). This project has received funding from the European Unions Framework Programme for Research and Innovation Horizon 2020 (2014-2020) under the Marie Skodowska−Curie Grant Agreement No. 745755. The computation was performed by the Infrastructure for the production and characterization of Nanomaterials, Biomaterials and Systems in Biomedice (ICTS NANBIOSIS), specifically by the High Performance Computing Unit of CIBER-BBN at University of Zaragoza.

Appendix A. Automatic artifact detection

The first Hjorth parameter (H_1) is defined as an estimation of the central frequency of the signal, and the second Hjorth parameter (H_2) as half of the bandwidth. For an intra-subject robustness analysis, a median adaptive filter was implemented using a 4-minutes window length to define $\widehat{H_1(n)}$ and $\widehat{H_2(n)}$. Empirical thresholds were used to determine whether a signal segment is considered as an artifact under following conditions:

$$H_2(n) > \underbrace{\widehat{H_2(n)} + T_2^u}_{\eta_2^u} \parallel H_1(n) > \underbrace{\widehat{H_1(n)} + T_1^u}_{\eta_1^u} \parallel H_1(n) < \underbrace{\widehat{H_1(n)} - T_1^l}_{\eta_1^l} \tag{A.1}$$

where $T_1^u = 1.4$ Hz, $T_1^l = 1$ Hz, $T_2^u = 1.7$ Hz for finger PPG and $T_2^u = 0.8$ Hz for forehead PPG.

The Hjorth parameters estimated for one PPG-transmission based signal are shown in Figures A1a and A1b. As an example of the artifact detector applicability, one artifact segment detected is shown in Figure A1c.

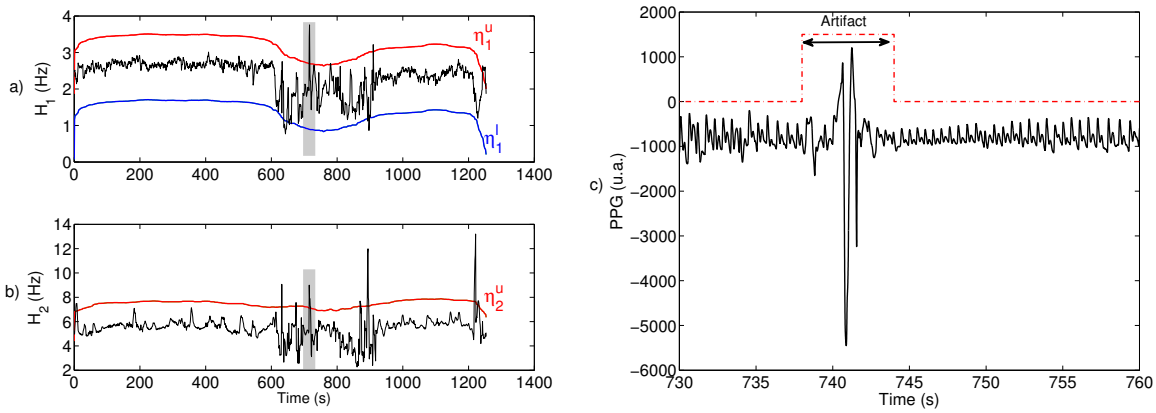

Figure A1: Hjorth parameters, (a) H_1 and (b) H_2, and related thresholds η estimated for one PPG-transmission based signal and, (c) one related artifact segment detected within the time-interval 730 to 760 seconds (shadow area).

References

Allen, J. et al. (2007), 'Photoplethysmography and its application in clinical physiological measurement', *Physiological measurement* **28**(3), R1.

Baek, H. et al. (2015), 'Reliability of ultra-short-term analysis as a surrogate of standard 5-min analysis of heart rate variability', *Telemedicine and e-Health* **21**(5), 404–414.

Bernardi, L. et al. (1997), 'Synchronous and baroceptor-sensitive oscillations in skin microcirculation: evidence for central autonomic control', *American Journal of Physiology-Heart and Circulatory Physiology,* **273**(4), 1867–1878.

Bland, J. et al. (1986), 'Statistical methods for assessing agreement between two methods of clinical measurement', *The Lancet* **1**(8476), 307–310.

Buxi, D. et al. (2015), 'A survey on signals and systems in ambulatory blood pressure monitoring using pulse transit time', *Physiological measurement* **36**(3), R1.

Charlot, K. et al. (2009), 'Interchangeability between heart rate and photoplethysmography variabilities during sympathetic stimulations', *Physiological measurement* **30**(12), 1357.

Chreiteh, S. et al. (2014), 'Sternal pulse rate variability compared with heart rate variability on healthy subjects', *Conf Proc IEEE Engineering in Medicine and Biology Society (EMBC)* pp. 3394–3397.

Fallow, B. et al. (2013), 'Influence of skin type and wavelength on light wave reflectance', *Journal of clinical monitoring and computing* **27**(3), 313–317.

Fisher, R. et al. (1925), 'Statistical methods for research workers', *Oliver Boyd* .

Gil, E. et al. (2008), 'Detection of decreases in the amplitude fluctuation of pulse photoplethysmography signal as indication of obstructive sleep apnea syndrome in children', *Biomedical Signal Processing and Control* **3**(3), 267–277.

Gil, E. et al. (2010), 'Photoplethysmography pulse rate variability as a surrogate measurement of heart rate variability during non-stationary conditions', *Physiological measurement* **31**(9), 1271.

Grajales, L. et al. (2006), 'Wearable multisensor heart rate monitor', *Wearable and Implantable Body Sensor Networks, BSN, International Workshop on. IEEE* .

Hemon, M. et al. (2016), 'Comparison of foot finding methods for deriving instantaneous pulse rates from photoplethysmographic signals', *Journal of clinical monitoring and computing* **30**(2), 157–168.

Khandoker, A. et al. (2011), 'Comparison of pulse rate variability with heart rate variability during obstructive sleep apnea', *Medical engineering and physics* **33**(2), 204–209.

Lazaro, J. et al. (2014), 'Pulse rate variability analysis for discrimination of sleep-apnea-related decreases in the amplitude fluctuations of pulse photoplethysmographic signal in children', *IEEE Journal of Biomedical and Health Informatics* **18**(1), 240–246.

Lin, L. et al. (1989), 'A concordance correlation coefficient to evaluate reproducibility', *Biometrics* **45**, 255–268.

Lu, G. et al. (2009), 'A comparison of photoplethysmography and ecg recording to analyse heart rate variability in healthy subjects', *Journal of medical engineering technology* **33**(8), 634–641.

Martinez, J. et al. (2004), 'A wavelet-based ecg delineator: evaluation on standard databases', *IEEE transactions on biomedical engineering* **51**(4), 570–581.

Mateo, J. et al. (2003), 'Analysis of heart rate variability in the presence of ectopic beats using the heart timing signal', *IEEE Transactions on Biomedical Engineering* **50**(3), 334–343.

McNames, J. et al. (2006), 'Reliability and accuracy of heart rate variability metrics versus ecg segment duration', *Medical and Biological Engineering and Computing* **44**(9), 747–756.

Niztan, M. et al. (1998), 'The variability of the photoplethysmographic signal-a potential method for the evaluation of the autonomic nervous system', *Physiological measurement* **19**(1), 93.

Pecchia, L. et al. (2018), 'Are ultra-short heart rate variability features good surrogates of short-term ones? state-of-the-art review and recommendations', *Healthcare Technology Letters* **5**(3), 94–100.

Peng, R. et al. (2015), 'Extraction of heart rate variability from smartphone photoplethysmograms', *Computational and mathematical methods in medicine* .

Peralta, E. et al. (2017), 'Robust pulse rate variability analysis from reflection and transmission photoplethysmographic signals', *Computing in Cardiology (CinC), 2017. IEEE* pp. 1–4.

Porto, L. et al. (2009), 'Comparison of time-domain short-term heart interval variability analysis using a wrist-worn heart rate monitor and the conventional electrocardiogram', *Pacing and Clinical Electrophysiology* **32**(1), 43–51.

Posada-Quintero, H. et al. (2013), 'Evaluation of pulse rate variability obtained by the pulse onsets of the photoplethysmographic signal', *Physiological measurement* **34**(2), 179.

Rajala, S. et al. (2017), 'Pulse arrival time (pat) measurement based on arm ecg and finger ppg signals-comparison of ppg feature detection methods for pat calculation', *Engineering in Medicine and Biology Society (EMBC), 2017 39th Annual International Conference of the IEEE* pp. 250–253.

Rhee, S. et al. (2001), 'Artifact-resistant power-efficient design of finger-ring plethysmographic sensors', *IEEE transactions on biomedical engineering* **48**(7), 795–805.

Salahuddin, L. et al. (2007), 'Ultra short term analysis of heart rate variability for monitoring mental stress in mobile settings', *Engineering in Medicine and Biology Society* pp. 4656–4659.

Salehizadeh, S. et al. (2015), 'A novel time-varying spectral filtering algorithm for reconstruction of motion artifact corrupted heart rate signals during intense physical activities using a wearable photoplethysmogram sensor', *Sensors* **16**(1), 10.

Schafer, A. et al. (2013), 'How accurate is pulse rate variability as an estimate of heart rate variability?', *International journal of cardiology* **166**(1), 15–29.

Spigulis, J. et al. (2005), 'Optical noninvasive monitoring of skin blood pulsations', *Applied optics* **44**(10), 1850–1857.

Tamura, T. et al. (2014), 'Wearable photoplethysmographic sensors—past and present', *Electronics* **3**(2), 282–302.

TaskForce (1996), *Task Force of the ESC-NASPE, Heart Rate Variability: Standards of Measurement, Physiological Interpretation, and Clinical Use, Circulation*, Vol. 17.

Vescio, B. et al. (2018), 'Comparison between electrocardiographic and earlobe pulse photoplethysmographic detection for evaluating heart rate variability in healthy subjects in short- and long-term recordings', *Sensors (Basel)* **18**(3), 844.

Wang, L. et al. (2007), 'Multichannel reflective ppg earpiece sensor with passive motion cancellation', *IEEE transactions on biomedical circuits and systems* **1**(4), 235–241.

Welch, P. et al. (1967), 'The use of fast fourier transform for the estimation of power spectra: a method based on time averaging over short, modified periodograms', *IEEE Transactions on audio and electroacoustics* **15**(2), 70–73.

Yao, J. et al. (2007), 'A pilot study on using derivatives of photoplethysmographic signals as a biometric identifier', *Engineering in Medicine and Biology Society, 2007. EMBS 2007. 29th Annual International Conference of the IEEE* pp. 4576–4579.

Yeragani, V. et al. (2007), 'Exaggerated differences in pulse wave velocity between left and right sides among patients with anxiety disorders and cardiovascular disease', *Psychosom. Med.* **69617**(2).

Zhang, Z. et al. (2014), 'Troika: A general framework for heart rate monitoring using wrist-type photoplethysmographic signals during intensive physical exercise', *IEEE Transactions on Biomedical Engineering* **62**(2), 522–531.